Available online at www.sciencedirect.com
SCIENCE DIRECT®
Inorganica Chimica Acta 357 (2004) 1168–1176
Inorganica Chimica Acta
www.elsevier.com/locate/ica

Synthesis, solid-state characterization and antimicrobial activities of three different polymorphs of a copper(II) complex with 4-isopropyltropolone (hinokitiol) ☆

Kenji Nomiya *, Akira Yoshizawa, Noriko C. Kasuga, Hironari Yokoyama, Shoko Hirakawa

Department of Materials Science, Faculty of Science, Kanagawa University, Tsuchiya, Hiratsuka, Kanagawa 259-1293, Japan

Received 8 July 2003; accepted 4 October 2003

Abstract

There exist at least three different polymorphs in the copper(II) complex [Cu(hino)$_2$] with a hinokitiol ligand (Hhino; 4-isopropyltropolone [1]). In addition to deep-green plate crystals **1a** and deep-green rod crystals **1b**, whose crystal structures have been recently reported, novel green needle crystals **1c** of [Cu(hino)$_2$] were found, the crystal structure of which was here determined by single-crystal X-ray analysis. Since only one crystal structure has been reported for the copper(II) complex [Cu(trop)$_2$] with a tropolone ligand (Htrop), the polymorphism found in the crystals of [Cu(hino)$_2$] would be due to the presence of the isopropyl group on the tropolone ring. The synthetic conditions giving the three polymorphs in good yields were found and the crystals were characterized with elemental analysis, FT-IR, TG/DTA and X-ray powder diffraction (XPD) measurements, as well as solution molecular weight measurements for **1a**. The solid-state magnetic behaviors or the temperature-dependent magnetic susceptibilities were measured with Superconductivity Quantum Interference Devices (SQUID): **1a** showed a weak ferromagnetic interaction, **1b** showed a paramagnetic nature with $S = 1/2$, while **1c** showed a weak antiferromagnetic interaction. The antimicrobial activities for selected bacteria, yeasts and molds were also measured in the water-suspension system: **1a** and **1b** showed no activity, while **1c** showed modest activities, and these activities were compared with those of the neutral Hino and the anionic hino$^-$ ligands.

Keywords: Copper(II) complex with hinokitiol; Crystal and molecular structures; Polymorphism; X-ray powder diffraction; Temperature-dependent magnetic susceptibilities; Antimicrobial activities

1. Introduction

The wide range of biological activities of hinokitiol (Hhino; $C_{10}H_{12}O_2$) [1], which is a 4-isopropyl substitution of tropolone (Htrop) [1] and is also called β-thujaplicin [2], is noteworthy; in fact, it shows a wide spectrum of antimicrobial activities against Gram-positive and -negative bacteria, yeasts and molds [3–7], and it is effective as a plant growth stimulator [8]. Of particular note is the fact that Hhino does not develop microorganisms-resistance [9,10], in contrast to many antibiotics. Other biological effects have been also observed, such as insecticidal activities [10], cytotoxic effect on the growth of mammalian cells and on blastogenesis of mouse splenic T cells [11], phytogrowth-inhibitory activities [12,13] and a function preventing discoloration in fresh animal and plant food [14]. Possibilities of the mode of action and mechanisms of hinokitiol have been proposed such as effective inhibitors of catechol-*O*-methyl transferase (COMT) [15] and effective scavenging activities against active oxygen species [16].

The monoanion of Hhino forms various metal-chelate complexes [M(hino)$_n$] through two unequivalent oxygen donor atoms [17], and it has been reported that

☆ Supplementary data associated with this article can be found, in the online version, at doi:10.1016/j.ica.2003.10.003.

* Corresponding author. Tel.: +81-463-59-4111; fax: +81-463-58-9684.
E-mail address: nomiya@chem.kanagawa-u.ac.jp (K. Nomiya).

[1] The systematic names for tropolone and 4-isopropyltropolone are 2-hydroxycyclohepta-2,4,6-trienone and 2-hydroxy-4-isopropylcyclohepta-2,4,6-trienone, respectively.

0020-1693/$ - see front matter © 2003 Elsevier B.V. All rights reserved.
doi:10.1016/j.ica.2003.10.003

their antimicrobial activities, in particular those of silver(I), iron(III) and copper(II) complexes, are significantly changed from that of Hhino [18]. We are interested in the structure–activity correlation in the antimicrobial activity of metal complexes with Hhino. However, X-ray structure analysis is so far limited to the several examples, i.e. of the "free" ligand Hhino [19], $[SnX_2(hino)_2]$ (X = F, Cl) [20], $[In(hino)_3]$ [21], $[Zn(hino)_2(EtOH)]_2$ [22], $[Cu(hino)_2]$ (Note: two polymorphs, **1a** and **1b**, have been structurally characterized [23]), and the very recently determined, dimeric silver(I) complex $[Ag(hino)]_2$, a dimeric cobalt(II) complex $[Co(hino)_2(EtOH)]_2$ and a monomeric aluminium(III) complex $[Al(hino)_3]\cdot MeOH$ [24], whereas there are considerable structural data of tropolonato-metal complexes [21,25–39], e.g. $[In(trop)_3]$ [21], [Na(trop)] [25,26], $[Th(trop)_4(DMF)]$ [27], $[SnCl(trop)_3]$ and $[Sn(OH)(trop)_3]$ [28], $[Fe(trop)_3]$ [29], $[Cu(trop)_2]$ [30–36], $[Al(trop)_3]$ [37], dimeric $[Co(4\text{-}Metrop)_2H_2O]_2$ plus monomeric $[Co(4\text{-}Metrop)_2]\cdot 2H_2O$ [38], and $[M(trop)_4]$ (M = Si, Ge, Sn)] [39].

In a separate account, the molecular structure of the coordinating $hino^-$ ligand is also interesting in comparison with that of the previously reported "free" Hhino ligand with the seven-membered 6π-conjugate system and without aromaticity [19,24].

In this work, we found the presence of novel green needle crystals **1c** of $[Cu(hino)_2]$ and determined the crystal structure by single-crystal X-ray analysis, in addition to the recently reported two polymorphs (deep-green plate crystals **1a** and deep-green rod crystals **1b**) [23]. The molecular structure of **1a** is comprised of a mixture of dimeric *trans*-, monomeric *trans*- and dimeric *cis*-forms, where the dimer/monomer is based on an intermolecular interaction through Cu···O interaction and the *cis*/*trans* is based on the relative position of the isopropyl groups (in **1a**, total ratio of the *trans*- and *cis*-forms is 3:2), and the molecular structure of **1b** consisted of only monomeric *trans*-form. Hence, there exist at least three different polymorphs in $[Cu(hino)_2]$, whereas only one crystal structure has been reported for $[Cu(trop)_2]$. Complexes **1a** and **1b** were quantitatively obtained by 2 h-refluxing of Hhino and $CuSO_4\cdot 5H_2O$ in different volumes of a mixed EtOH/water solvent. Complex **1c** was prepared using once isolated complexes **1a** or **1b** in the mixed EtOH/water solvent. The molecular structure of **1c** consisted of only monomeric *trans*-form, but the packing system was different from that of **1b**. These complexes showed different X-ray powder diffraction (XPD) patterns and different magnetic behaviors (temperature-dependent magnetic susceptibilities measurements with SQUID). Herein, we report full details of the synthesis, solid-state characterization of three different polymorphs (**1a–1c**), and the crystal and molecular structures of **1c**. Also reported are the antimicrobial activities for **1a–1c**, evaluated with minimum inhibitory concentration (MIC; μg mL^{-1}). Interestingly, these complexes in a water-suspension system showed different antimicrobial activities against selected bacteria, yeasts and molds.

2. Experimental

2.1. Reagents and methods

The following were reagent grade and used as received: $CuSO_4\cdot 5H_2O$, EtOH (Wako). The "free" ligand Hhino was supplied by Asahi Kasei Co., Japan.

CHN analyses were performed using a Perkin Elmer PE2400 series II CHNS/O Analyzer (Kanagawa University). Infrared spectra were recorded on a JASCO FT-IR 300 spectrometer as KBr disks at room temperature. Thermogravimetric (TG) and differential thermal analyses (DTA) were acquired using a Rigaku TG 8101D and TAS 300 data-processing system. TG/DTA measurements were run under air with a temperature ramp of 4 °C min^{-1} between 20 and 500 °C. The UV–Vis spectra were obtained using a JASCO V-560 spectrometer.

X-ray powder diffraction (XPD) data were collected on a Bruker M18XHF[22] diffractometer (Cu Kα radiation) at room temperature. Intensity data were collected by the step-counting methods (step 0.01° and sampling time 1.0 s) in the range $2\theta = 5$–60°.

The solid-state magnetic susceptibility measurement was performed in a quantum design SQUID susceptometer MPMS-55 in the temperature range 3–300 K with an applied field of 1 T. The data were corrected for the sample holder contribution and the diamagnetic contribution estimated through Pascal's constants.

Molecular weight measurements in solution based on the vaporimetric method (vapor pressure osmotic method) using vapor pressure osmometer were performed by Mikroanalytishes Labor Pascher (Remagen, Germany) and evaluated for 13.65 mg of the complex **1a** dissolved in 1.4905 g of chloroform.

ESR spectra at 297 K were obtained with a JEOL JES-RE2X X-band spectrometer. A chloroform solution of complex **1a** (10 mM) was placed in a Pyrex-quartz ESR tube with 5-mm inner diameter, degassed under 10^{-3} Torr, sealed, and used for measurement. X-Band ESR spectra at liquid nitrogen temperature (77 K) were also obtained with a JEOL JES-TE200. The *g* values were calibrated with Mn(II) marker used as a reference.

2.2. Synthesis of $[Cu(hino)_2]$

2.2.1. Deep-green plate crystals *1a*

To a colorless solution of 0.201 g (1.22 mmol) of Hhino dissolved in 30 mL of mixed EtOH and water

(1:1) solvent was added 0.155 g (0.62 mmol) of $CuSO_4 \cdot 5H_2O$, and the solution was refluxed for 2 h. The deep-green solution was passed through a folded filter paper (Whatman #2). The filtrate was evaporated slowly at room temperature. After a few days deep-green plate crystals were grown. They were collected on a membrane filter, washed with H_2O (50 mL × 3) and dried in vacuo. Deep-green plate crystals, insoluble in water and soluble in most organic solvents, were obtained in 70.7% (0.171 g scale) yield. *Anal*. Found: C, 61.71; H, 5.75. Calc. for $C_{20}H_{22}O_4Cu$ or [Cu(hino)$_2$]: C, 61.60; H, 5.69%. TG/DTA data: no weight loss was observed before decomposition. Decomposition began around 236 °C with an endothermic peak at 178 °C due to melting and an exothermic peak at 318 °C. Prominent IR bands (KBr disk): 2960vs, 2926s, 2865m, 1653m, 1635m, 1589vs (ν(C=O)), 1506vs (ν(C=C)), 1424vs, 1351vs, 1294s, 1238s (ν(C–O)), 1186m (ν(C–O)), 1130m, 1099w, 1075w, 1039m, 1020w, 958s, 937m, 915s, 894m, 877w, 817s, 776m, 740m, 666m, 580m, 511w, 429m cm^{-1}. The UV–Vis of **1a** (EtOH): λ_{max} 675 (ε 67) (d–d transition), 372, 338, 333 and 255 nm (broad and intense bands, which are probably due to π–π^* transition of the ligand).

2.2.2. Deep-green rod crystals *1b*

Synthesis of **1b** was different from that of **1a** only in the volume of the solvent; crystals **1b** was obtained from the reaction in 20 mL of mixed EtOH and water (1:1) solvent. Deep-green rod crystals, insoluble in water and soluble in most organic solvents, were obtained in 76.5% (0.185 g scale) yield. *Anal*. Found: C, 61.77; H, 5.72. Calc. for $C_{20}H_{22}O_4Cu$ or [Cu(hino)$_2$]: C, 61.60; H, 5.69%. TG/DTA data: no weight loss was observed before decomposition. Decomposition began around 220 °C with an endothermic peak at 179 °C due to melting and exothermic peaks at 353, 369 and 398 °C. Prominent IR bands (KBr disk): 2959vs, 2925m, 2864m, 1636m, 1590vs (ν(C=O)), 1577vs (ν(C=O)), 1509vs (ν(C=C)), 1462s, 1421vs, 1353vs, 1293s, 1237s (ν(C–O)), 1188m (ν(C–O)), 1140m, 1099w, 1074w, 1041m, 957s, 917s, 898m, 877w, 816s, 781m, 755m, 744s, 669m, 607m, 581m, 513w, 433m, 412w cm^{-1}.

2.2.3. Green needle crystals *1c*

Crystals of **1a** or **1b** (2.5 mmol) were redissolved in 20 mL of mixed EtOH/water (1:1) solvent, followed by 2 h-refluxing. The solution was concentrated to 15 mL using a rotary evaporator at 30–40 °C. After filtration through a folded filter paper (Whatman #2), the filtrate was allowed to stand in a refrigerator at 0 °C to give green needle crystals **1c** (65–76% yield). *Anal*. Found: C, 61.60; H, 5.75%. Calc. for $C_{20}H_{22}O_4Cu$ or [Cu(hino)$_2$]: C, 61.60; H, 5.69%. TG/DTA: no weight loss was observed below 220 °C. Endothermic peaks were observed at 178 (m.p.) and 336 °C, and exothermic peaks at 350, 364 and 386 °C. Prominent IR bands (KBr disk): 2955vs, 2930s, 2866m, 1636m, 1589vs(ν(C=O)), 1577vs (ν(C=O)), 1505vs(ν(C=C)), 1425vs, 1368vs, 1352vs, 1308m, 1274m, 1235s(ν(C–O)), 1186m(ν(C–O)), 1132w, 1076w, 1040w, 1021w, 957m, 912m, 887w, 808m, 781m, 745m, 666m, 582m, 511w, 433m cm^{-1}.

2.3. X-ray crystallography of green needle crystals *1c*

The intensity data were collected on a Bruker SMART APEX CCD diffractometer with Mo Kα radiation at 90 K using ω-scan. The structures were solved by direct methods followed by subsequent difference Fourier calculation and refined by a full-matrix least-squares procedure using program package SHELXTL [40]. All non-hydrogen atoms were refined anisotropically and hydrogen atoms isotropically. Crystal data for **1c**: $C_{20}H_{22}CuO_4$, M_r 389.92, triclinic, space group $P\bar{1}$(No. 1), $a = 5.0855(12)$ Å, $b = 6.9667(17)$ Å, $c = 13.681(3)$ Å, $\alpha = 77.626(3)°$, $\beta = 84.588(3)°$, $\gamma = 70.266(3)°$, $V = 445.52(19)$ Å^3, $Z = 1$, $D_{calcd} = 1.45$ Mg m^{-3}, 3164 reflections measured, 2190 ($[I > 2\sigma(I)]$) used in the refinement on F^2, $R = 0.0487$, $wR = 0.1162$.

2.4. Antimicrobial activity

Antimicrobial activities of the "free" ligand and the three polymorphs **1a–1c** in water-suspension system were evaluated by the MIC (μg mL^{-1}) as described elsewhere [41–46].

3. Results and discussion

3.1. Synthesis, compositional characterization and properties of three polymorphs of [Cu(hino)$_2$]

The two polymorphs of [Cu(hino)$_2$] have been prepared as deep-green plate crystals **1a**, comprised of dimeric *trans*-, monomeric *trans*- and dimeric *cis*-forms in the solid-state, and rod crystals **1b**, comprised of monomeric *trans*-forms in the solid-state [23]. In this work, complexes **1a** and **1b** were obtained in 71% and 75% yields, respectively, by 2:1 molar-ratio reaction of Hhino with $CuSO_4 \cdot 5H_2O$ under 2 h-refluxing conditions in mixed EtOH and water (1:1) solvent using 30 and 20 mL, respectively. On the other hand, novel green needle crystals **1c**, comprised of only monomeric *trans*-form in the solid-state, were obtained in 65–76% yield by 2 h-refluxing of crystals **1a** or **1b** (2.5 mmol) redissolved in 20 mL of mixed EtOH/water (1:1) solvent, followed by standing in a refrigerator at 0 °C. The three polymorphs of [Cu(hino)$_2$] with m.p. 179 °C, were insoluble in water, but soluble in most organic solvents, and decomposed at around 233 °C. Complex **1c** showed a tendency to change to **1b** after one month or more

standing at room temperature in the solid-state. XPD patterns were used to confirm the structure of **1a–1c** because the XPD patterns of **1a–1c** were markedly different from each other (see Section 3.2).

The molecular formulas of **1a–1c** with Cu^{2+}: $hino^- = 1:2$ composition and without any solvated molecules were consistent with elemental analysis and TG/DTA measurements. Molecular weight measurement of **1a** in $CHCl_3$ solution at room temperature, based on the vapor pressure osmotic method, showed 382 (Calcd value for $[Cu(hino)_2]$ was 389.9). This indicates that the dimeric structures contained in **1a** in the solid-state are dissociated and all complexes are present as a monomeric species in $CHCl_3$ solution, showing that both monomeric *cis*- and *trans*-forms probably exist in 2:3 molar ratio in solution.

The FT-IR spectra of **1a**–**1c** showed several characteristic bands due to the isopropyl group at 2960, 2928, 2866 cm^{-1}, ν(C=O) at 1589 and 1576 cm^{-1}, ν(C=C) at 1505 cm^{-1} and ν(C–O) at 1239 and 1187 cm^{-1}, which can be compared with those of Hhino, $[Na(hino)]\cdot 2H_2O$ [24], $[Zn(hino)_2]$ [22], $[Sn(hino)_2]$ and $[Zn(trop)_2]$ [22]. The UV–Vis absorption spectrum of **1a** in EtOH, consisting of the 675 nm band (ε 67) due to d–d transition and the broad and intense bands at 372, 338, 333 and 255 nm probably due to π–π^* transition of the ligand, was very similar to that of $[Cu(trop)_2]$ in EtOH [678, 377, 329, 246.3 nm] [30].

*3.2. Crystal and molecular structures of **1c**, and X-ray powder diffraction patterns of **1a–1c***

During a few days' standing of the mixed EtOH and water (1:1) solution in a refrigerator at 0 °C, crystals of **1c** with sufficient quality suitable for single-crystal X-ray diffraction studies were grown. The molecular and crystal structures of **1c**, with the atom numbering schemes, are depicted in Figs. 1 and 2. Selected bond distances and angles with their standard deviations are given in Table 1.

X-ray structure analysis of **1c** revealed that the crystal structure was composed of monomeric *trans*-form of the planar CuO_4 core with regard to the isopropyl groups (the sum of four angles around the Cu1 atom was 360°). The molecular structure of **1c** was very similar to that of **1b** (Fig. 1), but different from that of **1a** consisting of dimeric *trans*-, monomeric *trans*- and dimeric *cis*-forms. The Cu1 atom was sandwiched between two intermolecular tropolone rings ($C1^i$–$C7^i$ and $C11^{ii}$–$C17^{ii}$; symmetry operations i; $x+1, y, z$, ii; $x-1, y, z$) as a ladder-type stacking and the distance between Cu1 and one ring plane was 3.36 Å (Fig. 2). Such an intermolecular interaction is not observed in **1b**. These aspects are in contrast to that of $[Cu(trop)_2]$ with a transoid structure, which exists as a sandwich-type dimer by face-to-face stacking (3.3–3.8 Å) [30]. Within the tropolone

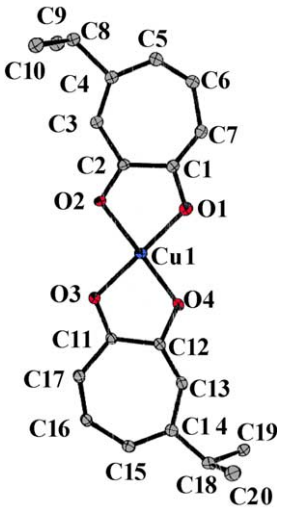

Fig. 1. ORTEP view of molecular structure of **1c** with the numbering scheme.

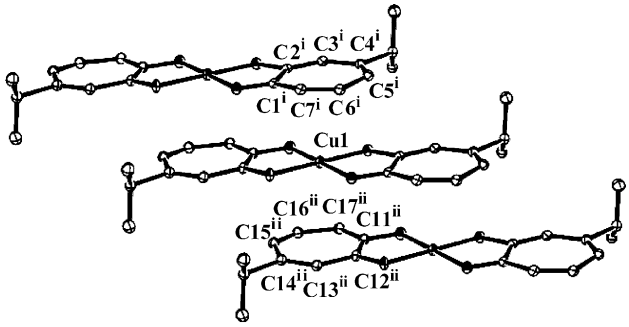

Fig. 2. Packing diagram of **1c** (symmetry operations i; $x+1, y, z$, ii; $x-1, y, z$).

Table 1
Selected bond distances (Å) and bond angles (°) for **1c**

Cu1–O1 1.885(12)	C6–C7 1.31(2)
Cu1–O2 1.928(12)	C1–C7 1.48(2)
Cu1–O3 1.952(11)	C11–O3 1.32(2)
Cu1–O4 1.881(13)	C12–O4 1.290(19)
C1–O1 1.29(2)	C12–C11 1.479(18)
C2–O2 1.308(19)	C12–C13 1.48(2)
C2–C1 1.466(17)	C13–C14 1.39(2)
C2–C3 1.33(2)	C14–C15 1.43(2)
C3–C4 1.41(2)	C15–C16 1.279(19)
C4–C5 1.37(2)	C16–C17 1.48(2)
C5–C6 1.496(17)	C11–C17 1.32(2)
O4–Cu1–O1 97.1(5)	O2–Cu1–O3 94.9(5)
O1–Cu1–O2 83.3(5)	O4–Cu1–O3 84.7(5)

rings of **1c**, the C1–C2 and C11–C12 bonds were essentially single bonds, and partial delocalization on the atoms of the ring was observed (the mean distance for the C3–C4, C5–C6, C7–C1, C12–C13, C14–C15 and C16–C17: 1.46 Å and for C2–C3, C4–C5, C6–C7, C13–C14,

C15–C16 and C17–C11: 1.33 Å). The distances of C1–O1, C2–O2, C11–O3 and C12–O4 (the mean distance: 1.30 Å) were almost the same, and these values are compared with an ordinal C=O distance (1.21 Å) and an ordinal C–O distance (1.36 Å). The two methyl groups of the isopropyl group were vertical to the ring plane in **1c** (Fig. 2). It has been concluded that neither Htrop nor Hhino possesses any appreciable degree of aromatic character [19,47,48]. The present work also rules out aromaticity of the coordinating hino$^-$ ligand in **1a–1c**.

X-ray power diffraction (XPD) patterns observed for **1a**–**1c** were markedly different from each other as shown in Fig. 3, and they were, therefore, useful for convenient determination of the three different crystal structures. The simulation of the powder pattern obtained by single-crystal X-ray analysis suggested the presence of

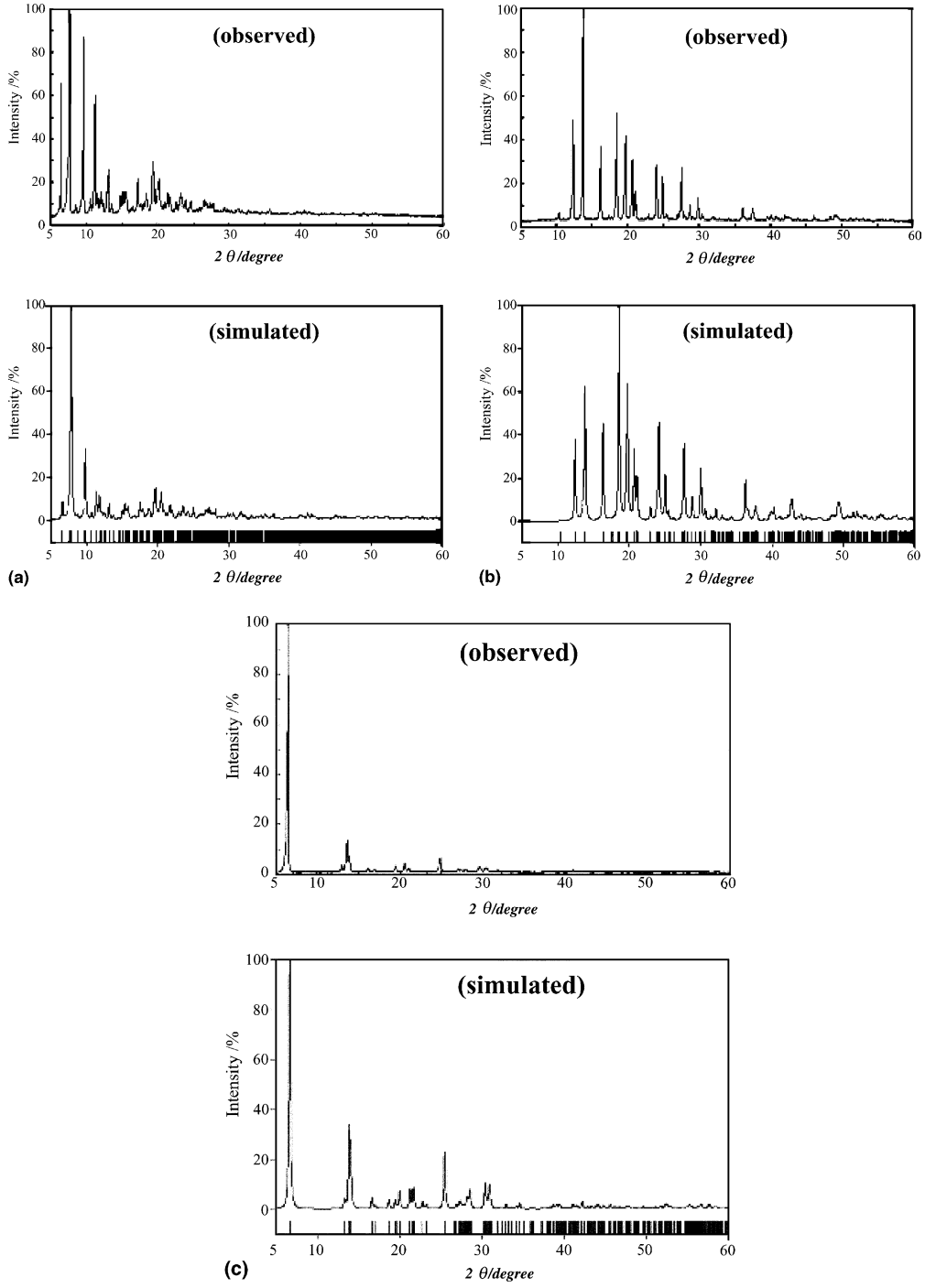

Fig. 3. The observed XPD patterns (above) and simulated patterns (below) derived from single-crystal X-ray diffraction data, in each set of pair of figures for plate crystals **1a**, rod crystals **1b** and needle crystals **1c**.

strong peaks 2θ at 6.68°, 7.82°, 9.69° for **1a**, 10.55, 12.44° for **1b**, and 6.62°, 13.88°, 19.48° for **1c**, respectively. The observed peaks 2θ were found at 6.49°, 7.66°, 9.60° for **1a**, 10.39°, 12.36° for **1b**, in which the peak intensities below 10° were small, and 6.43°, 13.91° and 19.50° for **1c**. Thus, the observed XPD patterns of **1a**–**1c** were in accord with the simulation patterns (Fig. 3) derived from the single-crystal X-ray diffraction data. These XPD patterns also indicate that the single crystals are representative of the bulk samples.

3.3. Magnetic susceptibility measurements of *1a–1c* and ESR spectra of *1a*

Temperature-dependent magnetic susceptibilities (χ_A) for **1a**–**1c** were measured with SQUID as plots of the observed values of χ_A and/or $1/\chi_A$, and μ_{eff} (or μ_B), versus temperature in the range of 3–300 K (Fig. 4). The magnetic behaviors were different from each other: **1a** showed a weak ferromagnetic interaction, **1b** showed a paramagnetic nature with $S = 1/2$, while **1c** showed a weak antiferromagnetic interaction [49–51].

The ESR parameters ($g_\perp = 2.049$, $g_{//} = 2.295$, $A_\perp = \pm 38 \times 10^{-4}$ cm^{-1}, $A_{//} = \pm 178 \times 10^{-4}$ cm^{-1}), evaluated from four-line ESR spectrum of **1a** measured in frozen $CHCl_3$ solution at 77 K, are compared with those of the previously reported data ($g_\perp = 2.036$, $g_{//} = 2.264$, $A_\perp = \pm 29 \times 10^{-4}$ cm^{-1}, $A_{//} = \pm 146 \times 10^{-4}$ cm^{-1}) for the square planar bis(acetylacetonato)copper(II) complex, [Cu(acac)$_2$] [52,53]. The differences in g and A values in the two copper(II) complexes may be attributed to the different geometries around the copper(II) centers, i.e. the rectangular CuO_4 core of **1a** versus the *almost complete* square planar CuO_4 core of [Cu(acac)$_2$] [54], and also to the different chelate-ring sizes based on the extended π-conjugate systems, i.e. 10-membered ring of **1a** (through O1–C1–C7–C6–C5–C4–C3–C2–O2 bond of hino$^-$ ligand) versus 6-membered ring of [Cu(acac)$_2$] (through O–C–C–C–O bond of acac$^-$ ligand).

3.4. Antimicrobial activities

Antimicrobial activities of complexes **1a**–**1c** prepared here, together with the "free" Hhino ligand and the sodium salt [Na(hino)]·2H$_2$O, are listed in Table 2, as estimated by the minimum inhibitory concentration (MIC; μg mL^{-1}).

Hhino showed a wide range of effective activities against bacteria, yeasts and molds, except for one

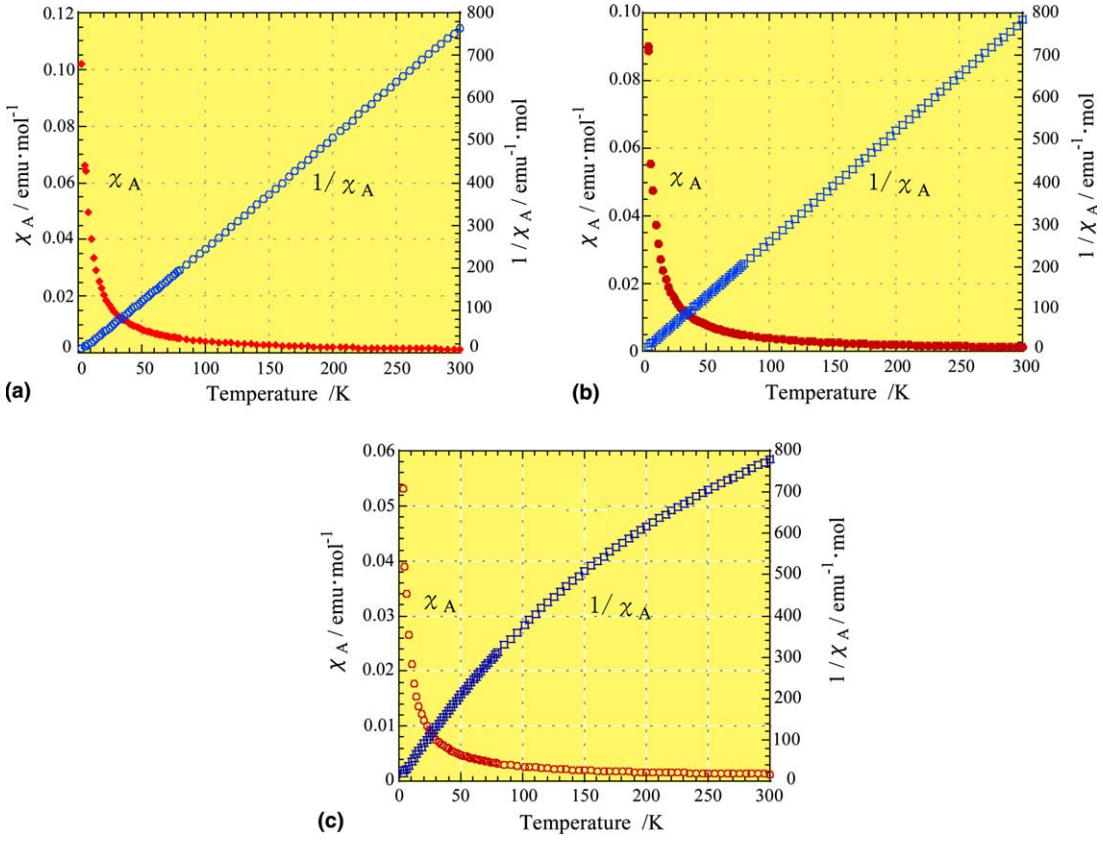

Fig. 4. Temperature-dependent magnetic susceptibility measurements (SQUID) of **1a**–**1c**.

Table 2
Antimicrobial activities evaluated by MIC (μg mL^{-1})

Test organism	Hhino	$[Na(hino)] \cdot 2H_2O$	$CuSO_4 \cdot 5H_2O$	**1a**	**1b**	**1c**[a]	
						(1)	(2)
Escherichia coli	250	62.5	>1000	>1000	1000	500	500
Bacillus subtilis	125	31.3	>1000	>1000	1000	500	500
Staphylococcus aureus	250	>1000		>1000	1000	250	62.5
Pseudomonas aeruginosa	1000	>1000		>1000	>1000	>1000	>1000
Candida albicans	62.5	7.9		>1000	>1000	1000	1000
Saccharomyces cerevisiae	62.5	7.9		>1000	>1000	500	1000
Aspergillus niger	62.5	15.7		>1000	>1000	500	1000
Penicillium citrinum	62.5	15.7		>1000	>1000	250	1000

[a] Results of repeat trials by **1c** with two different lot-numbers.

Gram-negative bacterium (*Pseudomonas aeruginosa*). The sodium salt $[Na(hino)] \cdot 2H_2O$, actually acting as an anionic $hino^-$ species [24], also showed a wide spectrum of antimicrobial activities, but a more subtle variety; it showed enhanced activities against two bacteria (*Escherichia coli* and *Bacillus subtilis*), two yeasts (*Candida albicans* and *Saccharomyces cerevisiae*) and two molds (*Aspergillus niger* and *Penicillium citrinum*), but it showed depressed activities against two bacteria (*Staphylococcus aureus* and *P. aeruginosa*). Thus, we can say that both neutral Hhino and anionic $hino^-$ molecules show noteworthy antimicrobial activities. The results are consistent with the reported data for other Gram-negative and Gram-positive bacteria [18]. The target of inhibition, the mechanism and mode of action have not been so far clarified, although several possibilities have been proposed [15,16].

Complexes **1a** and **1b** showed no activity against the same microbes, while complex **1c** showed a wide spectrum of modest activities against selected bacteria, yeasts and molds. The repeat trials for antimicrobial test by **1c** with two different lot-numbers exhibited the modest activities, showing the reproducibility. These results would be a first example of the antimicrobial activities that the crystal structure influences.

Here, it should be noted that the present results are different from the literature [18] that has reported higher activities of the copper(II) complex against several Gram-positive bacteria (*S. aureus* and *Enterococcus faecium*) and Gram-negative bacteria (*P. aeruginosa*) than Hhino and the sodium salt. The literature does not describe if the copper(II) complex used for the test is the crystals or the powder. One reason for the controversial results will be attributed to the purity of the complex used in the literature. In fact, the analytical data of the report showed the composition of Cu^{2+}: $hino^- = 1:1.77$ or 1.13:2 [18], suggesting that it is contaminated with a "free" copper(II) ion.

The aqueous copper(II) ion, i.e. $[Cu(H_2O)_n]^{2+}$ ion has shown antimicrobial activities, and there are proposed many mechanisms; most are concerned with interactions of copper(II) and/or copper(I) ions with DNA and protein, and a formation of a radical species such as ·OH generated by Fenton mechanism on the Cu^{2+}-bound biopolymer [55]. On the other hand, antimicrobial activities by copper(II) complexes have been scarcely studied and the mechanisms have not been reported.

The antimicrobial activities and solid-state properties show significant features. (1) Complexes **1a**–**1c** are an inert complex or stronger metal-oxygen bonding complex, and it is not dissociated in solution under evaluation of an antimicrobial test. If the complex is dissociated in solution, the activities by the "free" copper(II) ion and "free" $hino^-$ ion will appear. A formation of the CuO_4 core inhibits an interaction of oxygen atoms linked to C1 and C2 atoms with microorganisms/protein. (2) Depending on the solid-state packing manner, the hinokitiol–metal complex can show activities for selected microorganisms. An interaction of oxygen atoms linked to C1 and C2 atoms with microorganisms/protein may not be only a factor of antimicrobial activities.

4. Conclusions

Three different polymorphs **1a**–**1c** of $[Cu(hino)_2]$ have been prepared in good yields and characterized by XPD, FT-IR, TG/DTA and elemental analysis. The novel crystal structure of **1c** was determined by single-crystal X-ray analysis: **1c** was composed of a monomeric *trans*-form of the planar CuO_4 core with regard to the isopropyl groups. The molecular structure of **1c** was very similar to that of **1b**, but **1c** revealed a ladder-type stacking, which was not seen in the crystal of **1b**. Within the seven-membered ring with 6π-conjugate system, the C1–C2 bond was essentially a single bond (1.461(6) Å) and the π-electron system was completely delocalized on the atoms of the ring except the C1–C2 bond. Thus, the aromaticity of the coordinating $hino^-$ ligand was ruled out. Molecular weight measurements in $CHCl_3$ showed that the complex of **1a** was present as a monomer in solution, which probably contains 2:3-ratio of *cis*- and *trans*-forms.

As anticipated, the three polymorphs showed different magnetic properties; **1a** showed a weak ferromagnetic interaction, **1b** showed a paramagnetic nature, while **1c** showed a weak antiferromagnetic interaction. Complexes **1a** and **1b** showed no antimicrobial activities against selected microorganisms, but only **1c** showed a wide spectrum of antimicrobial activities. The antimicrobial test was performed in water suspension solution, but not in homogeneous solution, and these results would be a first example of the antimicrobial activities that the crystal structure influences. The presence of the 4-isopropyl group in the tropolone ring significantly influences the crystal structures of $[Cu(hino)_2]$, resulting in different effects on XPD, SQUID and antimicrobial activities. Thus, the polymorphism of crystals of other metal complexes with the $hino^-$ ligand will be also of interest. Studies in this direction are in progress and the data will be reported in due course.

5. Supplementary material

Supplementary crystallographic data sets for the structure of **1c** are available through the Cambridge Structural Data base [CCDC number 219712]. Copies of this information may be obtained free of charge from The Director, CCDC, 12 Union Road, Cambridge CB2 1EZ, UK (fax: +44-1223-336-033; e-mail: deposit@ccdc.cam.ac.uk or http://www.ccdc.cam.ac.uk).

Acknowledgements

Financial support by a Grant-in-Aid for Scientific Research (C) No. 10640552 and by a High-tech Research Center Project, both from the Ministry of Education, Culture, Sports, Science and Technology, Japan, is acknowledged. Financial support and a supply of Hhino by Asahi Kasei Co., Japan, are acknowledged. We thank Dr. K. Yoza, Bruker AXS Japan, for the structure analysis, Prof. W. Mori (Kanagawa University) for SQUID measurements and Dr. A. Minegishi for ESR measurements.

References

[1] T. Nozoe, Bull. Chem. Soc. Jpn. 11 (1936) 295.
[2] H. Erdtman, J. Gripenberg, Nature 161 (1948) 179.
[3] K. Okazaki, A. Homma, Yakugaku Zasshi (Japanese) 74 (1953) 174.
[4] Y. Taga, M. Ozaki, Sogo Igaku (Japanese) 12 (1955) 1106.
[5] S. Katsura, K. Tamura, S. Hatori, S. Maeda, Tohoku J. Exp. Med. (Japanese) 49 (1948) 357.
[6] I. Shibasaki, G. Terui, J. Ferement. Technol. (Japanese) 33 (1955) 216.
[7] T. Okabe, K. Saito, Y. Otomo, Fragr. J. (Japanese) 17 (1989) 74.
[8] A. Kafuku, Japan Kokai (1976) 7622819 [Chem. Abstr. 85 (1976) 15349z].
[9] S. Watanabe, Niigata Igaku Zasshi (Japanese) 67 (1953) 938.
[10] Y. Inamori, Y. Sakagami, Y. Morita, M. Shibata, M. Sugiura, Y. Kumeda, T. Okabe, H. Tsujibo, N. Ishida, Biol. Pharm. Bull. 23 (2000) 995.
[11] Y. Inamori, H. Tsujibo, H. Ohishi, F. Ishii, M. Mizugaki, H. Aso, N. Ishida, Biol. Pharm. Bull. 16 (1993) 521.
[12] Y. Inamori, K. Nishiguchi, N. Matsuo, H. Tsujibo, K. Baba, N. Ishida, Chem. Pharm. Bull. 39 (1991) 2378.
[13] Y. Sakagami, Y. Inamori, N. Isoyama, H. Tsujibo, T. Okabe, Y. Morita, N. Ishida, Biol. Pharm. Bull. 23 (2000) 645.
[14] R. Fukuzawa, T. Ito, Y. Matsuda, Japan Kokai Tokkyo Koho JP 60141244 [Chem. Abstr. 104 (1985) 104483p.].
[15] B. Belleau, J. Burba, J. Med. Chem. 6 (1963) 755.
[16] Y. Arima, A. Hatanaka, S. Tsukihara, K. Fujimoto, K. Fukuda, H. Sakurai, Chem. Pharm. Bull. 45 (1997) 1881.
[17] H. Iinuma, Nihon Kagakukai Shi (Japanese) 64 (1943) 742.
[18] S. Matsumoto, T. Fukui, S. Terasaki, S. Yoshinaka, A. Hasegawa, T. Okabe, K. Saito, K. Iinuma, J. Antibact. Antifung. Agents (Japanese) 22 (1994) 265.
[19] J.E. Derry, T.A. Hamor, J. Chem. Soc., Perkin II Trans. (1972) 694.
[20] M.C. Barret, M.F. Mahon, K.C. Molloy, P. Wright, Main Group Metal Chem. 23 (2000) 663.
[21] I. Abrahams, N. Choi, K. Henrick, H. Joyce, R.W. Matthews, M. McPartlin, F. Brady, S.L. Waters, Polyhedron 13 (1994) 513.
[22] M.C. Barret, M.F. Mahon, K.C. Molloy, J.W. Steed, P. Wright, Inorg. Chem. 40 (2001) 4384.
[23] M.C. Barret, M.F. Mahon, K.C. Molloy, P. Wright, J.E. Creeth, Polyhedron 21 (2002) 1761.
[24] K. Nomiya, A. Yoshizawa, K. Tsukagoshi, N.C. Kasuga, S. Hirakawa, J. Watanabe, J. Inorg. Biochem. (2003) in press.
[25] Y. Sasada, I. Nitta, Acta Crystallogr. 9 (1956) 205.
[26] R. Shino, Acta Crystallogr. 14 (1961) 42.
[27] V.W. Day, J.L. Hoard, J. Am. Chem. Soc. 92 (1970) 3626.
[28] J.J. Park, D.M. Collins, J.L. Hoard, J. Am. Chem. Soc. 92 (1970) 3636.
[29] T.A. Hamor, D.J. Watkin, J. Chem. Soc., Chem. Commun. (1969) 440.
[30] M. Hasegawa, Y. Inomaki, T. Inayoshi, T. Hoshi, M. Kobayashi, Inorg. Chim. Acta 257 (1997) 259.
[31] D.S. Ribeiro, A.V. Manuel, R.J. Irving, Bull. Chem. Soc. Jpn. 50 (1977) 734.
[32] L.G. Hulett, D.A. Thornton, Spectrochim. Acta Part A 29 (1973) 757.
[33] L.G. Hulett, D.A. Thornton, Spectrochim. Acta Part A 27 (1971) 2089.
[34] J.E. Berg, A.M. Pilotti, A.C. Soderholm, B. Karlsson, Acta Crystallogr. Sect. B34 (1978) 3071.
[35] G. Basu, Ind. J. Chem. 6 (1968) 453.
[36] H. Junge, Spectrochim. Acta Part A 24 (1968) 1957.
[37] E.L. Muetterties, L.J. Guggenberger, J. Am. Chem. Soc. 94 (1972) 8046.
[38] M.L. Post, J. Trotter, Acta Crystallogr. Sect. B 31 (1975) 1980.
[39] M. Kira, L.C. Zhang, C. Kabuto, H. Sakurai, Organometallics 17 (1998) 887.
[40] G.M. Sheldrick, SHELXTL-NT V6.1, Bruker AXS.
[41] K. Nomiya, H. Yokoyama, J. Chem. Soc., Dalton Trans. (2002) 2483.
[42] K. Nomiya, S. Takahashi, R. Noguchi, S. Nemoto, T. Takayama, M. Oda, Inorg. Chem. 39 (2000) 3301.
[43] K. Nomiya, S. Takahashi, R. Noguchi, J. Chem. Soc., Dalton Trans. (2000) 1343.
[44] K. Nomiya, K. Tsuda, T. Sudoh, M. Oda, J. Inorg. Biochem. 68 (1997) 39.

[45] K. Nomiya, K. Tsuda, Y. Tanabe, H. Nagano, J. Inorg. Biochem. 69 (1998) 9.
[46] K. Nomiya, S. Takahashi, R. Noguchi, J. Chem. Soc., Dalton Trans. (2000) 4369.
[47] D.J. Bertelli, T.G. Andrews Jr., J. Am. Chem. Soc. 91 (1969) 5280.
[48] D.J. Bertelli, T.G. Andrews Jr., P.O. Crews, J. Am. Chem. Soc. 91 (1969) 5286.
[49] L. Li, D. Liao, Z. Jiang, S. Yan, Inorg. Chem. 41 (2002) 1019.
[50] A. Asokan, P.T. Manoharan, Inorg. Chem. 38 (1999) 5642.
[51] D.E. Root, M.J. Henson, T. Machonkin, P. Mukherjee, T.D.P. Stack, E.I. Solomon, J. Am. Chem. Soc. 120 (1998) 4982.
[52] H.R. Gersmann, J.D. Swalen, J. Chem. Phys. 36 (1962) 3221.
[53] R.J. Myers, Molecular Magnetism and Magnetic Resonance Spectroscopy, Prentice-Hall, New Jersey, 1973.
[54] H. Koyama, Y. Saito, H. Kuroya, J. Inst. Polytec. Osaka City Univ. Ser. C. Chem. 4 (1953) 43.
[55] R.B. Thurman, C.P. Gerba, CRC Crit. Rev. Environ. Contr. 18 (1989) 295.